Journal of Power Sources 246 (2014) 198–203

Contents lists available at ScienceDirect

Journal of Power Sources

journal homepage: www.elsevier.com/locate/jpowsour

Three-dimensionally porous Fe_3O_4 as high-performance anode materials for lithium–ion batteries

Hao Wu, Ning Du, Jiazheng Wang, Hui Zhang, Deren Yang*

State Key Lab of Silicon Materials, Department of Materials Science and Engineering, Cyrus Tang Center for Sensor Materials and Applications, Zhejiang University, Hangzhou 310027, People's Republic of China

HIGHLIGHTS

- Fe_3O_4 layer was deposited on a Cu 3D porous current collector.
- The porous Fe_3O_4 electrodes show superior cyclability and rate capabilities.
- Enhanced performance is attributed to the advantages of the porous structure.

ARTICLE INFO

Article history:
Received 20 May 2013
Received in revised form
10 July 2013
Accepted 12 July 2013
Available online 20 July 2013

Keywords:
Iron oxide
Three-dimensional
Porous electrodes
Lithium–ion batteries

ABSTRACT

This paper describes the synthesis of three-dimensionally porous Fe_3O_4 via template-assisted and subsequent electrochemical deposition methods. When used as anode materials of lithium–ion batteries, the porous Fe_3O_4 electrodes show better cyclability and enhanced rate capabilities compared to planar Fe_3O_4 electrodes. The superior performance can be attributed to improved electrical contact, fast electron transport and good strain accommodation of the porous electrodes. The effect of the thickness of the porous Fe_3O_4 electrodes on the lithium–ion battery performance has also been investigated.

1. Introduction

Rechargeable lithium–ion batteries (LIBs) have been the most utilized power source for portable electronic devices [1,2]. Graphite-based materials are commonly used as anode materials in most commercial LIBs due to their low cost, high yield and long cycle life. However, their limited gravimetric capacity (372 mAh g^{-1}) has prompted intensive research for alternative anode materials with large capacity at low potentials for next-generation vehicles [3]. Since the discovery of transition metal oxides as anode materials of LIBs, much effort has been devoted to improve their capacity and rate capability [4–6]. In contrast to the intercalation mechanism, transition metal oxides show a reversible "conversion process" in which the transition metal oxides are reduced to small metal clusters which can facilitate the decomposition of Li_2O [4–6]. Among the transition metal oxides, Fe_3O_4 (magnetite) is cheap, nontoxic and environmentally benign, which is considered as one of the most promising electrode materials [5,7]. The electrochemical evaluation results have shown that Fe_3O_4 reacts with eight Li ions per formula unit with a theoretical specific capacity of ~926 mAh g^{-1} which is far beyond that of commercial graphite anodes [8–10]. Furthermore, Fe_3O_4 exhibits higher electronic conductivities compared with other transition metal oxides.

Nevertheless, application of Fe_3O_4-based materials in practical LIBs is hindered due to its low rate capability arising from kinetic limitations and poor cycling stability owing to severe agglomerations and drastic volume change during Li–ion insertion and extraction [5]. Various strategies have been pursued for the synthesis of Fe_3O_4 nanostructures to circumvent the above-mentioned obstacles and achieve enhanced electrochemical performance. For example, Taberna et al. prepared a self-supported Fe_3O_4/Cu nanoarchitectured electrode for LIBs, which delivered good rate capability [5]. Zhang and co-workers reported the carbon-coated Fe_3O_4 nanospindles synthesized by partial reduction of hematite nanospindles with high reversible capacity (~745 mAh g^{-1} at C/5) as well as enhanced cycling performance [11]. Wang et al. fabricated

* Corresponding author. Tel.: +86 571 87953190; fax: +86 571 87952322.
E-mail address: mseyang@zju.edu.cn (D. Yang).

0378-7753/$ – see front matter © 2013 Published by Elsevier B.V.
http://dx.doi.org/10.1016/j.jpowsour.2013.07.063

graphene-encapsulated Fe_3O_4 nanoparticles with 3D laminated structure, which exhibited a stable capacity of about 650 mAh g^{-1} with no noticeable fading for up to 100 cycles [12]. For all these studies, the improved electrochemical performances can be attributed to efficient buffering of volume change, fast electron transport and good electrical contact during cycling.

More recently, we demonstrated a new type of 3D nano-architectured porous Cu via a simple template-assisted method, which can support the Si-based materials to improve their cycling performance [13]. Herein, we apply the porous Cu to deposit Fe_3O_4 as anode materials of LIBs, which delivers excellent cyclability and enhanced rate capabilities compared to planar Fe_3O_4 electrodes. The effect of the thickness of the Fe_3O_4 on the performance has also been investigated.

2. Experimental section

2.1. Synthesis of the porous Fe_3O_4 electrodes

The synthesis of porous Cu structure is similar to our previous paper with small modification [13]. Briefly, monodispersed silica spheres were synthesized by a modified Stöber method [14]. Then, 500 μL of as-prepared silica–ethanol solution was dispersed on a pre-cleaned Cu substrate, which was subsequently spin-coated at 1000 rpm for 30 s. The thickness of this layer can be varied by repeating the spin-coating steps. The as-grown silica opal-like templates were annealed at 100 °C for 2 h under a low pressure before electrochemical deposition of Cu. The inverse-opal-like Cu current collector was achieved by cathodic electrodeposition from an electrolytic bath consisting of $CuSO_4 \cdot 5H_2O$ 100 g L^{-1}, $(NH_4)_2SO_4$ 20 g L^{-1}, diethylenetriamine (DETA) 40 mL L^{-1}, into the interstices between the piled silica nanospheres of the above-mentioned templates, with a LK2006A electrochemical work station. The electrodeposition of Cu was carried out under galvanostatic conditions at a constant current density of −3 mA cm^{-2}. After deposition for 5 min, the silica–Cu composites were then converted to copper inverse-opal-like current collector by chemically etching the silica in aqueous HF solution (10 wt%) for 30 min. The copper 3D nanoporous network was deposited with Fe_3O_4 by another electrodeposition process from an alkaline aqueous solution consisting of 0.09 M $Fe_2(SO_4)_3$, 2 M NaOH complexed with 0.1 M triethanolamine. The magnetite coating was produced under stirring at a constant current density ($j = -5$ mA cm^{-2}) using the same three-electrode cell as-described above at a fixed temperature of 50 °C. Four types of thickness-controlled electrodes were prepared for comparison by depositing time of 30, 60, 90 and 120 s, respectively.

2.2. Characterization and electrochemical measurement

The obtained samples were characterized by X-ray powder diffraction (XRD) with a Rigaku D/max-ga X-ray diffractometer with graphite monochromatized Cu Kα radiation ($\lambda = 1.54178$ Å). The morphology and structure of the samples were examined by a field emission scanning electron microscope (SEM HITACH S4800) with an energy-dispersive X-ray spectrometer (EDX).

Electrochemical measurements were performed by coin type cells (CR2025) which were assembled in an argon-filled glove box (Mbraun, labstar, Germany) by directly using the as-synthesized porous Fe_3O_4 structures as the positive electrode, a lithium metal foil as the negative electrode, and 1 M $LiPF_6$ electrolyte solution (in EC:DMC/1:1 in volume ratio). A galvanostatic cycling test of the assembled cells was carried out on a Land CT2001A system within the potential range of 0.01–3.0 V at various discharge/charge current densities. Cyclic voltammetry (CV) was conducted in the potential window of 0.01–3.0 V and a scan rate of 0.1 mV s^{-1} on an Arbin BT 2000 system.

3. Results and discussion

As shown in Fig. 1, the fabrication of the porous Fe_3O_4 electrodes involves three steps: 1) growth of silica opal-like templates on a Cu substrate; 2) Cu inverse-opal-like porous current collector synthesized by electrodeposition of Cu in the interstices of silica nanospheres and subsequent removal of templates by HF etching; 3) deposition of a Fe_3O_4 layer onto the porous copper structure via another electrodeposition.

Fig. 2 shows the morphological and compositional characterization of a porous Fe_3O_4 electrode deposited for 60 s. It can be seen that the as-synthesized Cu substrate shows the ordered porous structure of uniformly distributed holes with a diameter of ~200 nm (Fig. 2a). After the deposition of Fe_3O_4, most of the holes have been covered by a uniform layer and the diameters of the holes decrease (Fig. 2b). Fig. 2c shows the cross-sectional SEM image of the porous Fe_3O_4 electrode. As observed, not only the surface holes, but also the inner holes were injected by Fe_3O_4 due to the uniform electrodeposition which is different from the sputtering deposition [13]. Energy–dispersive X-ray (EDX) spectroscopy was carried out to verify the composition of the as-synthesized sample (Fig. 2d). Elements Cu, Fe and O are detected, which may come from the Cu current collector and Fe_3O_4 layer, respectively. Fig. 3 shows the XRD pattern of the as-synthesized sample, in which all peaks are consistent with those of the Fe_3O_4 phase (JCPDS No. 19-0629) in addition to the reflections owing to metallic copper, further confirming the deposition of Fe_3O_4 layer.

The CV curve of a 60 s deposition time porous Fe_3O_4 electrode is shown in Fig. 4a. The sharp peak located at about 0.7 V in the first discharge curve can be attributed to the conversion of Fe_3O_4 to Fe and the formation of amorphous Li_2O ($Fe_3O_4 + 8Li^+ + 8e^- \leftrightarrow 3Fe^0 + 4Li_2O$) as well as the irreversible reaction with electrolyte [12,15]. Meanwhile, two peaks at about 1.63 and 1.86 V are recorded in the anodic process, corresponding to the reversible oxidation of Fe^0 to Fe^{3+} [16]. In the subsequent cycles, both reduction and oxidation peaks are positively shifted. The difference in the potential of the cathodic peaks between the second and the first cycle is due to the structural modification of Fe_3O_4 and also the strain introduced in Fe_3O_4 during the first cycle caused by the lithium insertion and extraction [17,18]. On the other hand, the positive shift of the anodic peaks is ascribed to the polarization of the electrode in the first cycle [15]. Moreover, peak

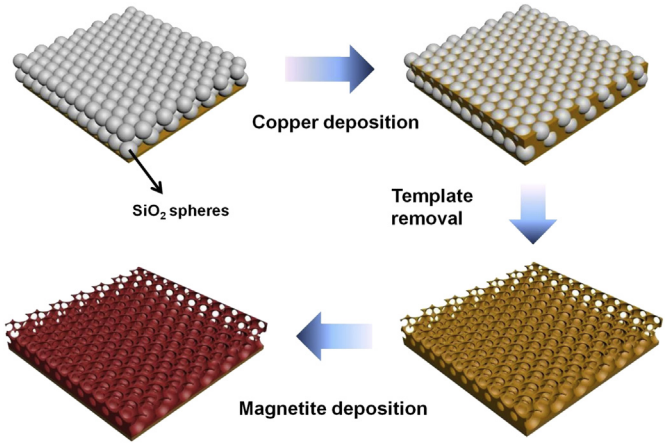

Fig. 1. Schematic of the fabrication process for porous Fe_3O_4 electrodes.